Journal of Alloys and Compounds 694 (2017) 24–29

Contents lists available at ScienceDirect

Journal of Alloys and Compounds

journal homepage: http://www.elsevier.com/locate/jalcom

Enhancement of critical current density by a "MgB_2-MgB_4" reversible reaction in self-sintered *ex-situ* MgB_2 bulks

Junming Peng [a], Qi Cai [a], Fang Cheng [a], Zongqing Ma [a, *], Chong Li [a], Ying Xin [b], Yongchang Liu [a, **]

[a] State Key Lab of Hydraulic Engineering Simulation and Safety, School of Materials Science & Engineering, Tianjin University, Tianjin 300072, People's Republic of China
[b] Tianjin University, Futong Group Research Center of Applied Superconductivity, Tianjin University, Tianjin 300072, People's Republic of China

ARTICLE INFO

Article history:
Received 5 August 2016
Received in revised form
10 September 2016
Accepted 28 September 2016
Available online 29 September 2016

Keywords:
MgB_2 superconductoro
Reversible reactiono
MgB_4o

ABSTRACT

Self-sintered *ex-situ* MgB_2 polycrystalline bulks have experienced a two-step sintering process, initially at 900 °C for 0–20 min and then at 650 °C for 1 h. MgB_2 was decomposed to MgB_4 and Mg at 900 °C and composed again at 650 °C from MgB_4 and Mg. The reversible reaction promotes the material migration, and thus eliminates pores and enhances the connectivity between the grains. The critical current density (J_c) is significantly improved due to both improved grain connectivity and the additive pinning centers such as MgB_4 and new-born boundaries. This two-step sintering process can be a promising method to fabricate high-performance *ex-situ* MgB_2 bulks and wires.

1. Introduction

MgB_2 is the intermetallic compound with a relatively high superconducting transition temperature of 39 K [1] and can be the most promising candidates for application in engineering without liquid helium [2], which also possesses the advantages such as 'weak-link free' grain coupling and low material cost. A great deal of work has been done to improve the superconducting properties, such as critical current density (J_c), the upper critical field (H_{c2}) and the irreversibility field (H_{irr}), of MgB_2. The introduction of additional flux pinning centers and connectivity enhancement of the grains are both necessary to increase the H_{irr} and the J_c to the levels required for commercial applications. As J_c is affected by the upper critical field, improvement in its H_{c2} is essential for practical applications of MgB_2. H_{c2} can be improved by the introduction of disorder through various processes such as chemical doping [3–7], irradiation [8] and various thermochemical processing techniques [9–11]. However, the relatively weak flux pinning in pure MgB_2 is the main factor of limitation in J_c especially under high fields [12], and recent studies have revealed that the current-transport properties in polycrystalline MgB_2 samples are considerably suppressed due to poor connectivity, reducing the effective current carrying cross-sectional area [13].

Two common methods are usually used for fabricating MgB_2 bulks and wires. The first is by using an *in-situ* reaction that starts with the heat treatment of mixed Mg and B powders. It is easy to add impurities to improve flux pinning in the *in-situ* method [14–16]. Since the chemical reaction between Mg and B forming MgB_2 results in about 30% volume reduction and porosity is known to be unavoidable during the *in-situ* process [17]. This inevitably results in a reduction of the engineering J_c. The second approach for fabricating MgB_2 bulks and wires is the *ex-situ* method. The *ex-situ* method that employs prereacted MgB_2 powder is favorable in terms of bulk density compared to the *in-situ* method [18]. A higher bulk density of 75% (the close-packing of rigid spheres) can be expected for the *ex-situ* method. However, grain connectivity in *ex-situ* MgB_2 bulks and wires was found to be worse than that of the *in-situ* fabricated MgB_2 samples [19]. It is attributed to the weak intergranular coupling and presence of impurities between the MgB_2 grains even after sintering at a high temperature of approximately 1100 °C [20]. Therefore, improving the intergranular coupling for *ex-situ* MgB_2 makes great sense in terms of fabrication of high-performance MgB_2 superconducting bulks and wires.

Previously, Tanaka et al. reported that the intergranular coupling strength of *ex-situ* MgB_2 could be significantly improved under

* Corresponding author.
** Corresponding author.
E-mail addresses: mzq0320@163.com (Z. Ma), licmtju@163.com (Y. Liu).

http://dx.doi.org/10.1016/j.jallcom.2016.09.312
0925-8388/

ambient pressure by heating at high temperature (900 °C) for a long period (100 h) [21]. As a consequence, the connectivity was far enhanced compared to that observed in conventional *ex-situ* MgB_2 samples. Another result showed that, the connectivity was further increased using high-purity laboratory-made MgB_2 with less surface oxidation and carbon-doped MgB_2 as starting powders [22]. Moreover, finer initial MgB_2 particle prepared by ball milling could account for the enhancement of intergranular coupling with both qualitative and quantitative [23]. Those results [21–23] also showed that only with long period sintering can the self-sintering among MgB_2 occur. All of their experiments were conducted in a sealed environment at a constant temperature, and the decomposition and composition of MgB_2 are not easy to achieve. They thought that the considerable evaporation of Mg and generation of MgB_4 when MgB_2 sample heated above 850 °C in an open system is the disadvantage of promotion of solid-state self-sintering.

In this paper, the *ex-situ* MgB_2 bulks were prepared by a reversible reaction through a two-step sintering process with the aim of improving the poor grains connectivity. It was found that the nature of self-sintering is material migration. Reversible reaction among MgB_2 bulks could promote the material migration. Moreover, we draw conclusions about the influence of two-step sintering process to the formation of new particles and the new heating method to the superconducting properties. This two-step sintering process can be a promising method to manufacture high-performance *ex-situ* MgB_2 bulks and wires.

2. Experimental procedure

Commercial magnesium diboride powders (99% purity, 30–100 μm in size) used in present work were from Alfa Aesar Chemicals Co. Ltd. The pure powder was pressed into cylindrical pellets with 5 mm in diameter and 1.5 mm in thickness under a pressure of 10 MPa. The pressed pellets were sintered at 900 °C varying from 0 to 20 min and then at 650 °C for 1 h under flowing high-purity Ar gas. All the heating programs were conducted in differential thermal scanners apparatus (Mettler Toledo, TGA/DSC 1 HT/1611). To reduce the Mg loss during the reversible reaction, pure Mg (3% of the weight of MgB_2) was laid up around the sample before heating. In this study, bulk samples are denoted by sintering temperature and sintering time. For example, a bulk sample only with 1 h preservation at 650 °C is called '650 °C, 1 h'; sample with 0 min preservation at 900 °C and then with 1 h preservation at 650 °C is called '900 °C, 0 min - 650 °C, 1 h'; sample with 10 min preservation at 900 °C and then with 1 h preservation at 650 °C is called '900 °C, 10 min - 650 °C, 1 h'; sample with 20 min preservation at 900 °C and then with 1 h preservation at 650 °C is called '900 °C, 20 min - 650 °C, 1 h'.

The phase composition and microstructure of the prepared samples were examined by the powder X-ray diffraction (XRD, D/MAX-2500) with Cu Kα radiation, scanning electron microscopy (SEM, Hitachi Model No.S 4800) and transmission electron microscopy (TEM, JEM-2100), respectively. Then the temperature dependence of resistivity in the sintered samples was measured by a DC four-probe method in the temperature range from 5 to 300 K. The magnetization of the sintered samples was measured using a physical properties measurement system (PPMS) at 20 K. J_c was calculated from the width of magnetization hysteresis loops (ΔM), based on the extended Bean model $J_c = 20\Delta M/a\,(1 - a/3\,b)$, where $\Delta M = M^+ - M^-$ is the hysteresis loop width and a and b ($a<b$) are the dimensions of a rectangular sample.

3. Results and discussion

The XRD results presented in Fig. 1 show that all samples

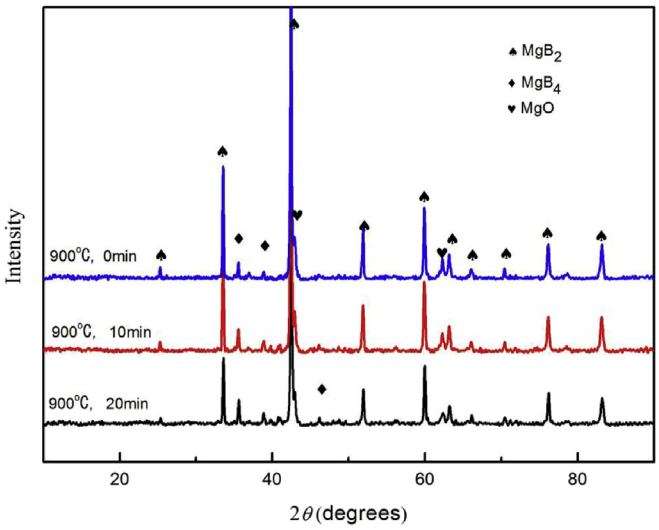

Fig. 1. XRD patterns of the MgB_2 bulks of different preservation time at 900 °C.

synthesized by one-step sintering contain MgB_2 as the dominant phase, and as the preserving time increases, the peak intensity of MgB_4 increases. The weight fraction of MgB_4 in these samples after one-step sintering was estimated based on the XRD data, and the corresponding value are 2.54%, 4.40% and 6.16% for sample '900 °C,0 min', sample '900 °C, 10min' and sample '900 °C, 20min', respectively. One can see that the amount of formed MgB_4 increases obviously with the preserving time prolonging. The main reason is the decomposition of MgB_2 with the product of MgB_4 at 900 °C ($MgB_2(s) \rightarrow MgB_4(s)+Mg(g)$) [24,25] has occurred and the decomposition goes in depth as time prolonged. The intensity of the Mg is too weak to recognize in Fig. 1 because of the Mg evaporation. Fig. 2 also shows that all samples synthesized by two-step sintering contain MgB_2 as the dominant phase. But compared with one-step sintered samples, the difference is that the intensity of MgB_4 decreases (sample '900 °C, 20 min - 650 °C, 1 h') and even vanishes (sample '900 °C,0 min - 650 °C, 1 h'; sample '900 °C, 10 min - 650 °C, 1 h'). The decreasing amount of the MgB_4 is the evidence of composition between MgB_4 and Mg (main from the

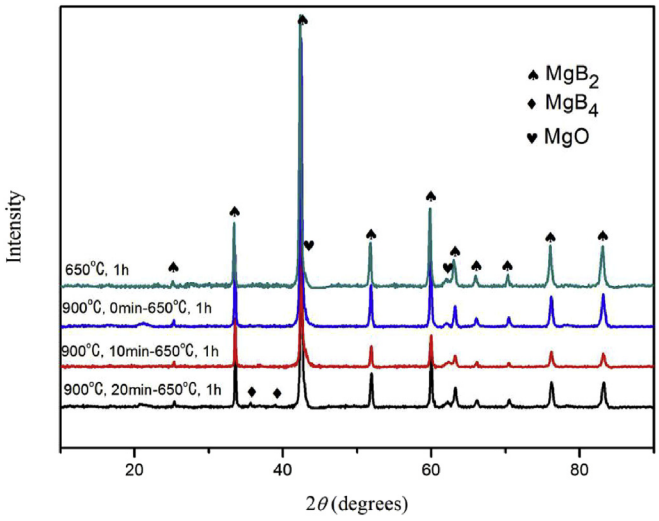

Fig. 2. XRD patterns of the MgB_2 bulks of different preservation time at 900 °C and then with 1 h preservation at 650 °C.

addition of Mg laid out of bulks) with the product of MgB_2 during the 1 h preservation period at 650 °C.

Fig. 3 presents typical microstructural features of MgB_2 polycrystalline bulks prepared by *ex-situ* with different heating programs. Here, gray, black, and white contrasts in the secondary electron images correspond to MgB_2 grains, pores, and impurity phases such as MgO, respectively. Fig. 3 a, sample '650 °C, 1 h', clearly shows microstructure with many pores between the particles. Obviously, it is owing to deficient self-sintering of *ex-situ* MgB_2. One can also see that the intergrain coupling of sample '650 °C, 1 h' (Fig. 3 a) between MgB_2 grains/particles is poor in contrast with that of sample '900 °C,0 min - 650 °C, 1 h', '900 °C, 10 min - 650 °C, 1 h', and '900 °C, 20 min - 650 °C, 1 h' (Fig. 3 b, c, d), in which more strongly linked MgB_2 grains are observed. We can also learn that as the preservation time prolonged at 900 °C, the intergrain coupling enhanced and the boundaries become vaguer (Fig. 3 b, c, d). All of these suggested that solid-state self-sintering occurred during the heat treatment.

Fig. 4 shows schematic diagrams of self-sintering of three grains [21], which can describe the results obtained from the different sintering programs properly in present work. Stage I (corresponding to sample '650 °C, 1 h') is the early stage of sintering and contact angle of grains becomes shallower (formation of necks) at this stage. The obvious characteristic of this stage is the reserve of many open pores. We can confirm this phenomenon from Fig. 3 a. At this stage, MgB_2 grains can hardly been decomposed because of low temperature, but the surface of grains has changed to form necks which are result from slow migration of MgB_2 at 650 °C. In the next stage (stage II, corresponding to sample '900 °C,0 min −650 °C, 1 h' and sample '900 °C, 10 min - 650 °C, 1 h'), pores are gradually eliminated by the formation of new grain boundaries (The detailed information of new boundary will be shown in Fig. 5 and discussed later). At this stage, the surface contact area increased and the bulk became denser. Fig. 3 b (sample '900 °C,0 min −650 °C, 1 h') and Fig. 3 c (sample '900 °C, 10 min - 650 °C, 1 h') show this situation appropriately. At the first step of this stage, MgB_2 grains begin to decompose to Mg and MgB_4, meanwhile Mg vapor can migrate easily to the areas with the low vapor pressure (for example necks and small pores). At the second step (650 °C for 1 h) of this stage, composition between Mg and MgB_4 occurs and new boundary forms. Moreover, Fig. 3 c shows better connectivity and the smaller pore than Fig. 3 b because of extra 10-min preservation at 900 °C and more MgB_2 particles being taken part in the reversible reaction. Given this, it's not difficult to explain Fig. 3 d (sample '900 °C, 20 min - 650 °C, 1 h') which is depicted by stage III hold the best connectivity which with 20 min preservation at 900 °C. At this stage III, more MgB_2 is decomposed and reformed, the original surface become closer and closer, pores are eliminated progressively and the new boundary formed at last. However, some unreacted MgB_4 and new-formed MgO are wrapped around the new-born boundary which can damage the connectivity. Isolated and closed pores and large grains can be seen in Fig. 3 d.

The HRTEM images of the sample '900 °C, 20 min - 650 °C, 1 h' are shown in Fig. 5. The new-born boundary was found between MgB_2 grains (as marked by a white line in Fig. 5b), and MgB_4 and MgO were recognized within the new-born boundary in Fig. 5 a. The corresponding lattice was confirmed by FFT (Fast Fourier Transformation). The decomposition of MgB_2 is easier to occur close to gaps and pores than in the particle center because gaps and pores can provide a highway for new formed Mg diffusing from original matrix, then some Mg may react with O_2 which exists in pores and gaps forming MgO. From Fig. 5 a, the scale of MgB_4 crystalline grains was measured varying 5–10 nm and those grains can act as flux pinning centers. When heating at 650 °C, pores and gaps are gradually eliminated and substituted by the new-born boundary. This also agrees with the stage IV in Fig. 4. The new-born boundary was built up by the unreacted MgB_4, impurity MgO, and new formed MgB_2. The width of this boundary was measured varying 10–15 nm.

According to the Rowell connectivity analysis, the active cross-sectional area fraction (A_F) represents the connectivity factor between adjacent grains [26,27]. Here the A_F is estimated as:

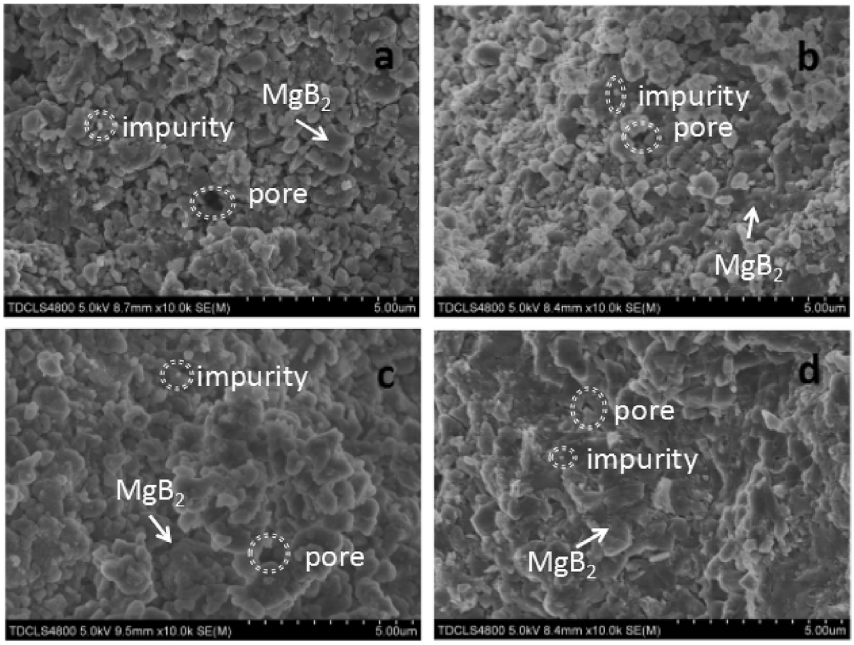

Fig. 3. SEM images of the sintered MgB2 bulks of (a) 1 h preservation at 650 °C, (b) preservation 0 min at 900 °C and then with 1 h preservation at 650 °C, (c) preservation 10 min at 900 °C and then with 1 h preservation at 650 °C, (d) preservation 20 min at 900 °C and then with 1 h preservation at 650 °C.

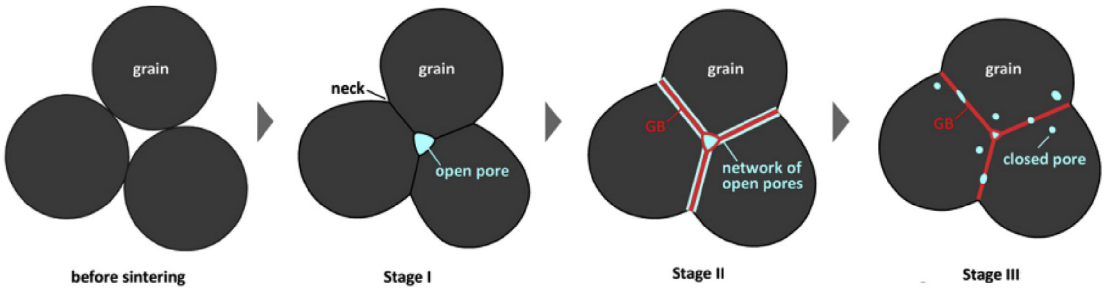

Fig. 4. Schematic diagrams of self-sintering of three grains which can describe the different results obtained from the sintering programs properly. Stage I: early stages of sintering; a contact angle of grains becomes shallower (formation of necks). Stage II: the middle stage of sintering; further evolution of necks and pores diffuse through and accumulate at grain boundaries (GBs). Stage III: the final stage of self-sintering; some pores are eliminated and isolated and closed pores appear [21]. The contact GB area between grains progressively increases and densification occurs during sintering.

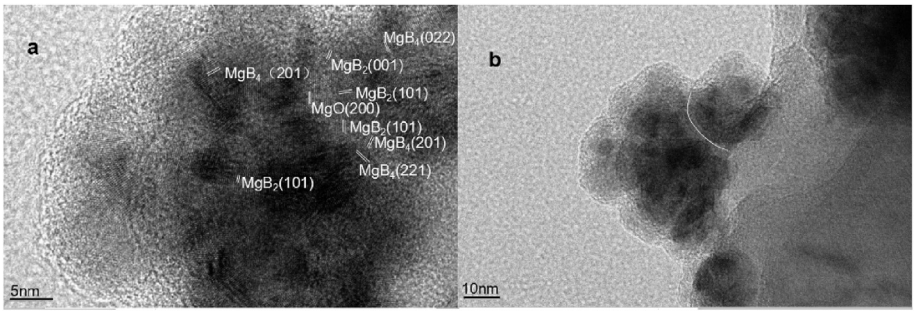

Fig. 5. HRTEM images for self-sintered MgB_2 sample '900 °C, 20 min - 650 °C, 1 h'.

$$A_F = \Delta\rho_{ideal}/(\rho_{300K} - \rho_{40K}) \quad (1)$$

$$\Delta\rho_{ideal} = \rho_{ideal(300K)} - \rho_{ideal(40K)} \quad (2)$$

Where ρ_{ideal} is the resistivity of a reference crystal and ρ_T is the measured resistivity. According to previous studies [27], here the $\Delta\rho_{ideal}$ is 7.3 $\mu\Omega$*cm. The results are listed in Table 1. The A_F values suggest that the connectivity of these samples increased as the duration time prolonged at 900 °C. However, the value of A_F for all the *ex-situ* samples are lower than that of *in-situ* samples, implying worse grain connectivity in *ex-situ* samples. This result is consistent with previous studies [19–21], where intergranular coupling of *ex-situ* MgB_2 samples was reported to be generally lower than *in-situ* ones due to the impurity phase at grain boundaries and the low bulk density. Actually, how to improve the grain connectivity of *ex-situ* MgB_2 sample is always a great challenge and also one of the research hotspots in terms of MgB_2 application. To further analyze the intergrain connectivity, the residual resistivity ratio (RRR) was also estimated (see Table 1). The value of RRR increases from sample '900 °C, 0 min - 650 °C, 1 h' to '900 °C, 20 min - 650 °C, 1 h'. These results also indicate that samples with longer preservation at 900 °C possess much better grain connectivity than the typical MgB_2 grains. Fig. 6 shows the resistivity versus temperature plots of sintered MgB_2 bulks with different preservation time at 900 °C and then with 1 h preservation at 650 °C. The resistivity of samples sintered at high temperature is lower than sintered at low

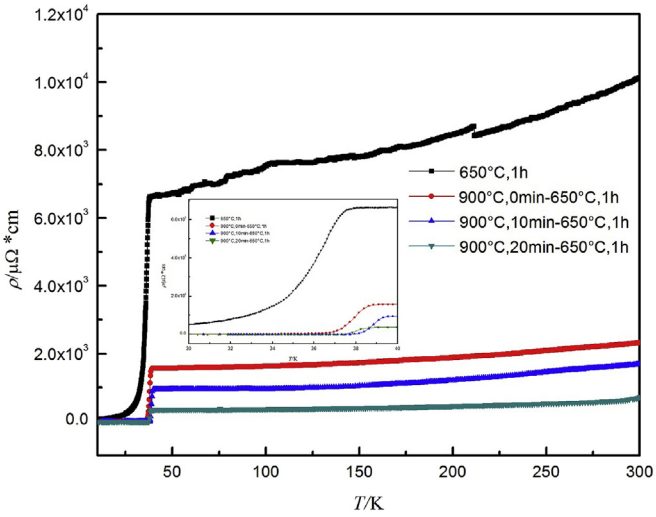

Fig. 6. The temperature dependence of resistivity of sintered MgB_2 bulks with different preservation time at 900 °C and then with 1 h preservation at 650 °C.

Table 1
T_c and electrical resistivity properties of sintered MgB_2 bulks with different preservation time at 900 °C and then with 1 h preservation at 650 °C.

Sample	T_c(K)	ρ_{300K} ($\mu\Omega$*cm)	ρ_{40K} ($\mu\Omega$*cm)	$\Delta\rho$($\mu\Omega$*cm)	A_F	RRR
650 °C, 1 h	37.4	10116.4	6650.2	3466.2	0.0021	1.92
900 °C, 0 min–650 °C, 1 h	38.7	2329.6	1571.6	758.0	0.0096	1.48
900 °C, 10 min–650 °C, 1 h	39.2	1598.0	946.9	651.1	0.0112	1.68
900 °C, 20 min–650 °C, 1 h	38.7	740.0	362.6	377.6	0.0193	2.04

temperature and as the duration time at 900 °C prolonged, the resistivity decreased significantly.

Fig. 7 shows the magnetic field dependence of J_c for all samples. It is particularly noteworthy that self-sintering can improve J_c across all the measured magnetic field. J_c of three one-step sintered samples without heating at 650 °C are all lower than that of two-step sintered samples with heating at 650 °C not only at the self-field but also at high fields. This phenomenon is explained by that one-hour preservation at 650 °C can reduce MgB_4 and enhance the connectivity, as discussed above. It was also found that J_c under self-field increases as the duration time prolonged at 900 °C. The improvement of J_c under self-field is attributed to the increase of coupling between grains, as discussed above and shown in Figs. 3 and 4. This is believed to contribute significantly to an effective path for the transport current in the superconducting states [20]. We can also note that J_c of sample ' 650 °C, 1 h' is a little higher than the sample '900 °C, 0 min - 650 °C, 1 h' at the self-field. However, this situation reversed at high fields because of the grown effective pinning centers such as new-born boundaries and MgB_4 [28] in sample '900 °C, 0 min - 650 °C, 1 h'. The value of J_c is still lower than the best values reported in previous studies [21,22], and there are two main reasons for this result. Firstly, due to our limited experimental condition, the inevitable impurity such as MgO scattered in the grains boundary degrade the value of J_c significantly. Then another more important reason is the intrinsic low connectivity of ex-situ sintered MgB_2 bulks despite some improvement by prolonging the duration time at 900 °C as discussed above. It can be boldly predicted that longer duration at 900 °C could result in more material migration and the improvement of connectivity.

Fig. 8 shows the normalized flux pinning force $f = F_p/F_{pmax}$ as a function of the reduced field $h = H/H_{irr}$ at 20 K for these *ex-situ* samples. Here, the flux pinning force F_p is calculated by the equation $F_p = \mu_0 H J_c$ ($\mu_0 = 4\pi^*10^{-7}$), F_{pmax} is the maximum value of $F_p(H)$, and H_{irr} is defined as the field at J_c = 100 A cm^{-2} [21]. In present study, the peak of F_p/F_{pmax} in the sample '650 °C, 1 h' and sample ' 900 °C, 0 min - 650 °C, 1 h' is located at about $h = 0.2$, which indicates that the grain boundary pinning is the predominant pinning mechanism in these samples [29]. And compared to the sample '650 °C, 1 h', the peak of sample '900 °C, 0 min - 650 °C, 1 h' moved to high fields. Besides, the original grain boundary and impurity, the new-born boundaries and the MgB_4 formed by the reversible reaction may also act as effective pinning centers. Moreover, we also can note that peaks of sample '900 °C, 10 min - 650 °C, 1 h' and sample '900 °C, 20 min - 650 °C, 1 h' shifted to higher fields and the sample '900 °C, 20 min - 650 °C, 1 h' to the highest fields. At this stage, more new-born boundaries and MgB_4 impurity can act as effective pinning centers. This agrees with the curves trend in Fig. 6 that at high fields the J_c was increased as the duration time prolonged at 900 °C.

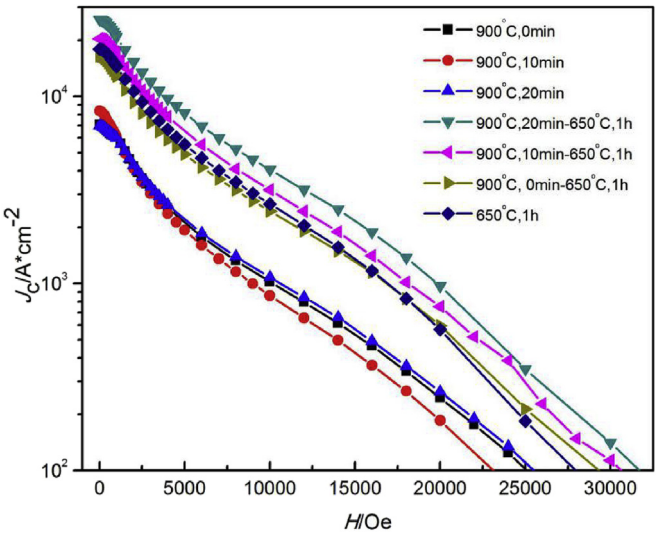

Fig. 7. Measured J_c-H characteristics of the sintered MgB_2 bulks with different preservation time at 900 °C and then with 1 h preservation at 650 °C.

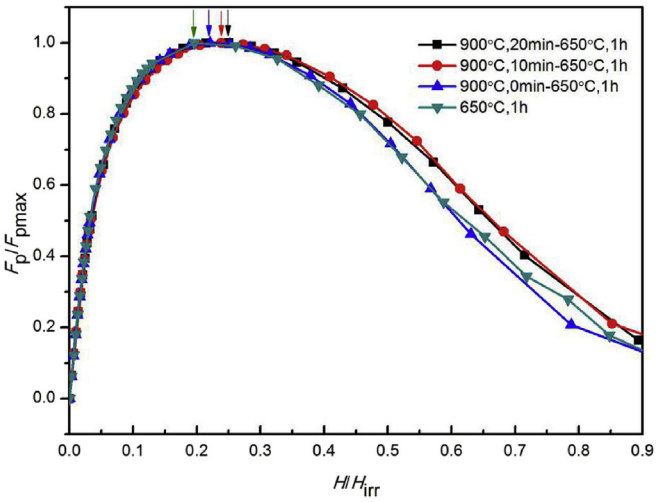

Fig. 8. Normalized pinning force F_p/F_{pmax} as a function of reduced magnetic field $h = H/H_{irr}$ at 20 K for the ex-situ sintered MgB_2 bulks with different preservation time at 900 °Cand then with 1 h preservation at 650 °C.

4. Conclusions

To improve the grain connectivity of *ex-situ* MgB_2 polycrystalline bulks, we attempted to take advantage of the decomposition of MgB_2 at relatively high temperature (900 °C) and then of the composition between MgB_4 and Mg at relatively low temperature (650 °C) with the product of MgB_2. By prolonging the preservation time (from 0 to 20 min) at high temperature, the decomposition was promoted and thus the amount of MgB_4 was increased. By heating at relatively low temperature (650 °C) for 1 h, MgB_2 has formed again and the amount of MgB_4 was decreased. This reverse reaction can promote material migration and thus enhance the connectivity. It's the critical factor for the enhancement of connectivity. The value of J_c was not only improved at the self-field but also at high fields. The reasons for these results are the connectivity between MgB_2 grains was enhanced, and also the new-born grain boundary and the impurity (MgB_4) served as effective pinning centers at high field. The employment of this reversible reaction is a promising method to fabricate high-performance *ex-situ* MgB_2 bulks and wires.

Acknowledgement

The authors are grateful to China National Funds for Distinguished Young Scientists (Grant No. 51325401), the National Natural Science Foundation of China (Grant No. 51302186 and 51574178) and the Natural Science Foundation of Tianjin (Grant No.14JCQNJC03300). This work is also supported by the National Magnetic Confinement Fusion Energy Research Project (grant No.2014GB125006).

References

[1] J. Nagamatsu, N. Nakagawa, T. Muranka, Y. Zeniranim, J. Akimitsu, Superconductivity at 39 K in magnesium diboride, Nature 410 (2001) 63–64.
[2] M. Eisterer, Magnetic properties and critical currents of MgB_2, Supercond. Sci. Technol. 20 (2007) R47.
[3] S.X. Dou, O. Shcherbakova, W.K. Yoeh, et al., Mechanism of enhancement in electromagnetic properties of MgB_2 by nano SiC doping, Phys. Rev. Lett. 98 (2007) 097002.
[4] S.X. Dou, S. Soltanian, J. Horvat, X.L. Wang, S.H. Zhou, M. Ionescu, H.K. Liu, P. Munroe, M. Tomsic, Enhancement of the critical current density and flux pinning of MgB_2 superconductor by nanoparticle SiC doping, Appl. Phys. Lett. 81 (2002) 3419.
[5] R.H.T. Wilke, S.L. Bud'ko, C. Canfield, D.K. Finnemore, R.J. Suplinskas, S.T. Hannahs, Systematic effects of carbon doping on the Superconducting properties of $Mg(B_{1-x}C_x)_2$, Phys. Rev. Lett. 92 (2004) 217003.
[6] H. Kumakura, H. Kitaguchi, A. Matsumoto, H. Hatakeyama, Upper critical fields of powder-in-tube-processed MgB_2/Fe tape conductors, Appl. Phys. Lett. 84 (2004) 3669.
[7] J.H. Kim, W.K. Yeoh, M.J. Qin, X. Xu, S.X. Dou, The doping effect of multiwall carbon nanotube on MgB_2/Fe superconductor wire, J. Appl. Phys. 100 (2006) 013908.
[8] M.D. Sumption, M. Bhatia, M. Rindfleisch, M. Tomsic, S. Soltanian, S.X. Dou, Large upper critical field and irreversibility field in MgB_2 wires with SiC additions, Appl. Phys. Lett. 86 (2005) 092507.
[9] Y. Bugoslavsky, G.K. Perkins, X. Qi, L.F. Cohen, A.D. Caplin, Enhancement of the high-magnetic field critical current density of superconducting $MgB_2$by proton irradiation, Nature 410 (2001) 561.
[10] R. Fluiger, H.L. Suo, N. Musolino, C. Beneduce, P. Toluemode, P. Lezza, Superconducting properties of MgB_2 tapes and wires, Phys. C 385 (2003) 286–305.
[11] A. Matsumoto, H. Kumakura, H. Kitaguchi, H. Hatakeyama, Effect of SiO_2 and SiC doping on the powder-in-tube processed MgB_2 tapes, Supercond. Sci. Technol. 16 (2003) 926–930.
[12] D.K. Finnemore, J.E. Ostenson, S.L. Bud'ko, G. Lapertot, P.C. Canfield, Thermodynamic and transport properties of superconducting $Mg^{10}B_2$, Phys. Rev. Lett. 86 (2001) 2420–2422.
[13] J.M. Rowell, The widely variable resistivity of MgB_2 samples, Supercond. Sci. Technol. 16 (2003) R17–R27.
[14] S.X. Dou, S. Soltanian, J. Horvat, X.L. Wang, S.H. Zhou, M. Ionescu, H.K. Liu, P. Munroe, M. Tomsic, Enhancement of the critical current density and flux pinning of MgB_2 superconductor by nanoparticle SiC doping, Appl. Phys. Lett. 81 (2002) 3419–3421.
[15] M. Mustapic, J. Horvat, M.S. Hossain, Z. Su, Z. Skoko, D. Mitchell, S.X. Dou, Novel synthesis of superparamagnetic Ni–Co–B nanoparticles and their effect on superconductor properties of MgB_2, Acta. Mater. 70 (2014) 298–306.
[16] J.H. Kim, S. Oh, Y.U. Heo, S. Hata, H. Kumakura, A. Matsumoto, M. Mitsuhara, S. Choi, Y. Shimada, M. Maeda, J.L. MacManus-Driscoll, S.X. Dou, Microscopic role of carbon on MgB_2 wire for critical current density comparable to NbTi, NPG Asia Mater. 4 (2012) E3.
[17] A. Yamamoto, J. Shimoyama, K. Kishio, T. Matsushita, Limiting factors of normal-state conductivity in superconducting MgB_2 : an application of mean-field theory for a site percolation problem, Supercond. Sci. Technol. 20 (2007) 658–666.
[18] Y. Shimada, S. Hata, K. Ikeda, H. Nakashima, S. Matsumura, H. Tanaka, A. Yamamoto, J. Shimoyama, K. Kishio, Microstructural Characteristics of ball-milled self-sintered ex situ MgB_2 bulks, Trans. Appl. Supercond. 25 (2014) 6801105.
[19] A. Yamamoto, H. Tanaka, J. Shimoyama, H. Ogino, K. Kishio, T. Matsushita, Towards the realization of higher connectivity in MgB_2 conductors: in-situ or sintered ex-situ? Jpn. J. Appl. Phys. 51 (2012) 010105.
[20] C.E.J. Dancer, P. Mikheenko, A. Bevan, J.S. Abell, R.I. Todd, C.R.M. Grovenor, A study of the sintering behaviour of magnesium diboride, J. Eur. Ceram. Soc. 29 (2009) 1817–1824.
[21] H. Tanaka, A. Yamamoto, J. Shimoyama, H. Ogino, K. Kishio, Strongly connected *ex-situ* MgB_2 polycrystalline bulks fabricated by solid-state self-sintering, Supercond. Sci. Technol. 25 (2012), 115022. (7pp).
[22] S. Mizutani, A. Yamamoto, J. Shimoyama, H. Ogino, K. Kishio, Understanding routes for high connectivity in ex situ MgB_2 by self-sintering, Supercond. Sci. Technol. 27 (2014), 044012 (7 pp.).
[23] S. Mizutani1, A. Yamamoto, J. Shimoyama, Hiraku Ogino1, Kohji Kishio, Self-sintering-assisted high intergranular connectivity in ball-milled ex situ MgB_2 bulks, Supercond. Sci. Technol. 27 (2014), 114001 (8pp).
[24] S. Brutti, A. Ciccioli, G. Balducci, G. Gigli, Vaporization thermodynamics of MgB_2 and MgB_4, Appl. Phys. Lett. 80 (2002) 2892.
[25] R. Schmitt, J. Glaser, T. Wenzel, K.G. Nickel, H.J. Meyer, A reactivity study in the Mg–B system reaching for an improved synthesis of pure MgB_2, Phys. C 436 (2006) 38–42.
[26] J.M. Rowell, S.Y. Xu, X.H. Zeng, A.V. Pogrebnyakov, Q. Li, X.X. Xi, J.M. Redwing, W. Tian, X. Pan, Critical current density and resistivity ofMgB_2 films, Appl. Phys. Lett. 83 (2003) 102–104.
[27] R.H.T. Wilke, S.L. Bud'ko, P.C. Canfield, D.K. Finnemore, R.J. Suplinskas, S.T. Hannahs, Synthesis and optimization of Mg(B1-xCx)2wire segments, Phys. C 424 (2005) 1–16.
[28] Q. Cai, Y.C. Liu, Z.Q. Ma, H.J. Li, L.M. Yu, Variation of pinning mechanism and enhancement of critical current density in MgB_2 bulk containing self-generated coherent MgB_4 impurity, Appl. Phys. Lett. 103 (2013) 132601.
[29] D. Hughes, The role of grain boundaries in determining J_c in high-field high-current superconductors, Philos. Mag. B 55 (1987) 459.